Progress In Electromagnetics Research Letters, Vol. 74, 39–45, 2018

Multiple-Arm Dipoles Reader Antenna for UHF RFID Near-Field Applications

Kui Jin, Jingming Zheng*, Xiaoxiang He, Yang Yang, Jin Gao, and Chun Zhou

Abstract—A multiple-arm dipoles antenna array based on magnetic coupling is proposed for ultra-high frequency (UHF) radio frequency identification (RFID) near-field application. The design utilizes four multiple-arm dipoles to form a square region fed by a quarter-wave impedance transformer double-side parallel stripline (QDSPSL) structure. Broadband performance can be obtained for two different resonant frequencies caused by different dipole arm lengths. Moreover, in induction area, stronger and more uniform magnetic field distribution is generated for phases of currents on three dipole arms being kept in the same compared to conventional single-arm dipole. A $170 \times 170 \times 1.6\,\text{mm}^3$ antenna has been fabricated on an FR-4 substrate to fit RFID near-field application. The measured 10-dB impedance bandwidth is 190 MHz (810–1000 MHz), which covers the entire UHF RFID frequency band (860–960 MHz). Measured tests on the antenna read range are carried out, exhibiting a reading region of $100 \times 100\,\text{mm}^2$ and 100% reading rate within 200 mm for near-field tags.

1. INTRODUCTION

Radio frequency identification (RFID) technologies based on magnetic coupling for ultra-high frequency (UHF) operations have been developed rapidly in the near-field item-tracking applications such as bottles of water, retail goods, and pharmaceuticals [1, 2]. As internal component of RFID systems, near-field reader antenna is required to generate strong and uniform distribution of magnetic field. Apart from this, licensed UHF bands are allocated within the 860 MHz to 960 MHz, so broadband performance of the antenna meeting different standards is necessary. Reference [3] gives a method to obtain strong H-field by four power-divider-fed single-arm dipoles, while the bandwidth is narrow (840–845 MHz). An electrically large zero-phase-shift line grid-array antenna is presented in [4]. It has a wide bandwidth and larger interrogation zone, however the 100% read percentage is achieved within 13.5 mm. [5] proposes dual-printed-dipoles for UHF RFID applications. In the design, the two printed dipoles compose a loop to provide in-phase current performance, and reading range is 37 mm (with Impinj UHF button). The antenna of Reference [6] can be applied well in near-field application and also achieve strong magnetic field, while the read distance is just 105 mm with an input power of 25 dBm. In addition, [7] achieves the broadband with taper structure, the antenna is also designed by single-arm dipole, at the center of which the magnetic field is lower than other places and field strength is below $-5\,\text{dBA/m}$ with an input power of 30 dBm. In Reference [8], although circular-polarised antenna is proposed for RFID application. The magnetic field in near-field is weak and non-uniform and read range for near-field tag is just 35 mm. Besides, some other antennas such as planar antenna for opposite directed currents [9, 10], complementary split ring resonator (CSRR) elements loading [11] and antenna with configurable reading area [12] are also adopted for UHF RFID near-field application and the bandwidth is narrow.

Received 9 January 2018, Accepted 8 March 2018, Scheduled 18 March 2018

* Corresponding author: Jingming Zheng (15895936277@163.com).

The authors are with the College of Electronic and Information Engineering, Nanjing University of Aeronautics and Astronautics (NUAA), Nanjing 210016, China.

In this letter, a multiple-arm dipoles antenna array for UHF near-field applications is proposed and analyzed by ANSYS HFSS electromagnetic simulation software. Four straight multiple-arm dipoles form a square region where strong and uniform magnetic can be achieved. Phases of currents on the arms of the proposed dipole are kept in the same and that causes superposition of magnetic field in interrogation zone. Different arm lengths of multiple-arm dipole also bring different resonant frequencies, so broadband performance of the antenna can be obtained. Measured tests are carried out in terms of antenna read range for near-field tags. Large reading region of $100 \times 100\,\text{mm}^2$ and 100% reading rate within 200 mm for near-field tags are exhibited. Measured performance in terms of reflection coefficient and tag detection is presented as follows.

2. ANTENNA LAYOUT AND PERFORMANCE

The proposed array antenna is composed of 4 straight multiple-arm dipoles fed by QDSPSL structure, printed on a 1.6 mm-thick FR-4 substrate with a dielectric constant of 4.4 and a loss tangent of 0.02 (Fig. 1). Coaxial probe is adopted at the center of the antenna to feed multiple-arm dipoles. Length of one arm of dipole is less than $\lambda/2$ ($L1$ is set as 101 mm in the design), and parameter of other two dipole arms is $L2$. Currents on three dipole arms are kept in phase and strong magnetic field can be generated over antenna surface. Besides, parameter $L1$ and $L2$ influence the resonant frequency. This because different dipole arm lengths cause different resonant frequencies and broadband performance is achieved. Double-side parallel stripline (QDSPSL) based on impedance transformers is introduced to match the input impedance (50 Ω) and also avoid radiation influence caused by itself for magnetic field on upper and lower surface counteracting. Feed arm lengths include two different parameters, one of which is set as $\lambda/4$ wavelength ($G1 = 48$ mm) and the other parameter $G2$ is to achieve better impedance matching and obtain large reading region for near-field tags. Antenna configuration and parameters are as follows (Fig. 1). Main geometrical parameters are: $L = W = 170$ mm, $L1 = 101$ mm, $L2 = 44$ mm, $G1 = 48$ mm, $G2 = 27$ mm, $W1 = 5$ mm, $W2 = 3.5$ mm and $R = 10$ mm.

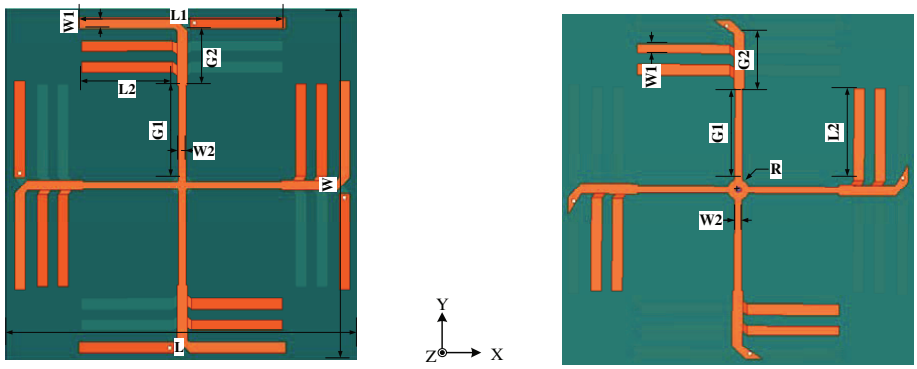

Figure 1. Antenna prototype (a) top view, (b) bottom view.

The antenna reflection coefficient is shown in Fig. 2. It is below −10 dB between 810 MHz–1000 MHz covering the whole UHF band. In the design, parameter $L1$ is different from parameter $L2$ and this causes different resonant frequencies separately at 850 MHz and 980 MHz. So broadband performance of the antenna can be achieved.

Figure 3 shows the simulated current distribution of the proposed antenna at 900 MHz. As can be seen, currents along three loops are kept in phase. Such current distribution generates strong and uniform magnetic field over the interrogation zone.

Vertical magnetic field ($|Hz|$, dBA/m) distributions at the height of 10 mm respectively along X and Y-axes are given in Fig. 4. The input power is 1 W. As seen, compared to the conventional single-arm dipole antenna array [6], the proposed multiple-arm dipole antenna array can achieve stronger and more uniform magnetic field over antenna surface. The field strength of the proposed antenna is

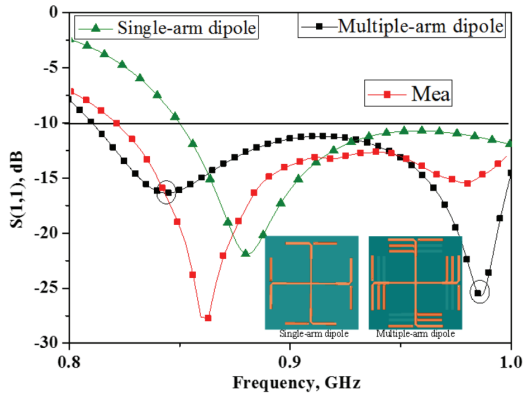

Figure 2. Reflection coefficient of proposed antenna compared to single-arm dipole.

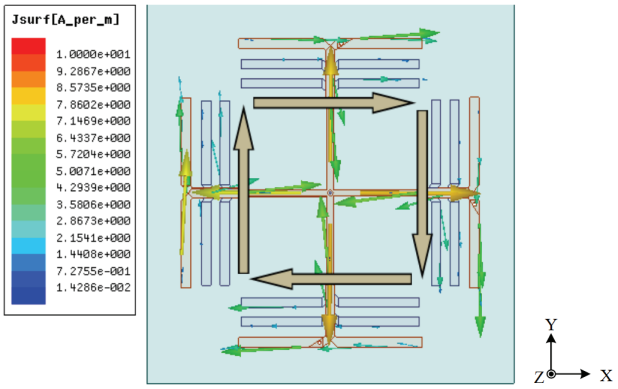

Figure 3. Antenna currents distribution at 900 MHz.

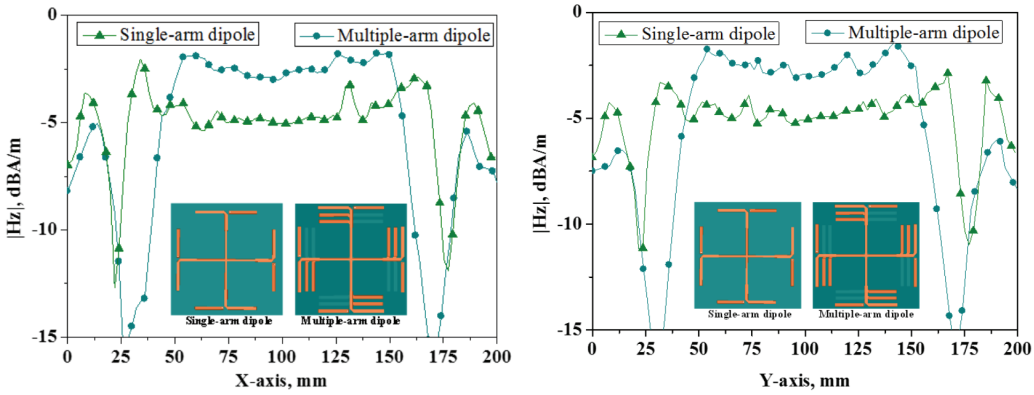

Figure 4. Simulated $|Hz|$ (dBA/m) compared to single-arm dipole at $Z = 10\,\text{mm}$ separately along X and Y-axis (a) X-axis, (b) Y-axis.

above $-2.5\,\text{dBA/m}$ in the interrogation zone ($50\,\text{mm} \leq X \leq 150\,\text{mm}$, $50\,\text{mm} \leq Y \leq 150\,\text{mm}$), while the field of single-arm dipole antenna array is below $-5\,\text{dBA/m}$. Although interrogation zone gets smaller than induction zone of conventional dipole array ($37.5\,\text{mm} \leq X \leq 162.5\,\text{mm}$, $37.5\,\text{mm} \leq Y \leq 162.5\,\text{mm}$), field strength is enhanced obviously. Such magnetic field distribution can achieve longer read range for near-field tags. Currents on three arms of the proposed dipole are kept the same, and this causes superposition of magnetic field in interrogation zone. Besides, out of the zone, field strength is lowered for magnetic field between dipole arms counteracting as currents kept in the same. And this avoids misreading of other near-field tags out of zone.

Quarter-wave impedance matching structure is adopted in the antenna. The formula for the quarter-wave transformer is known as:

$$Z_c = \sqrt{Z_{in}}\sqrt{R_L} \tag{1}$$

$$Z_c = \text{transformer characteristic impedance} \tag{2}$$

$$Z_{in} = \text{input impedance} \tag{3}$$

$$R_L = \text{terminal load.} \tag{4}$$

In this proposed antenna, the input impedance $Z_{in} = 50\,\Omega$, $R_L = 36\,\Omega$, and the calculated transformer characteristic impedance value is:

$$Z_c = \sqrt{50 \times 36} = 42.4\,\Omega \tag{5}$$

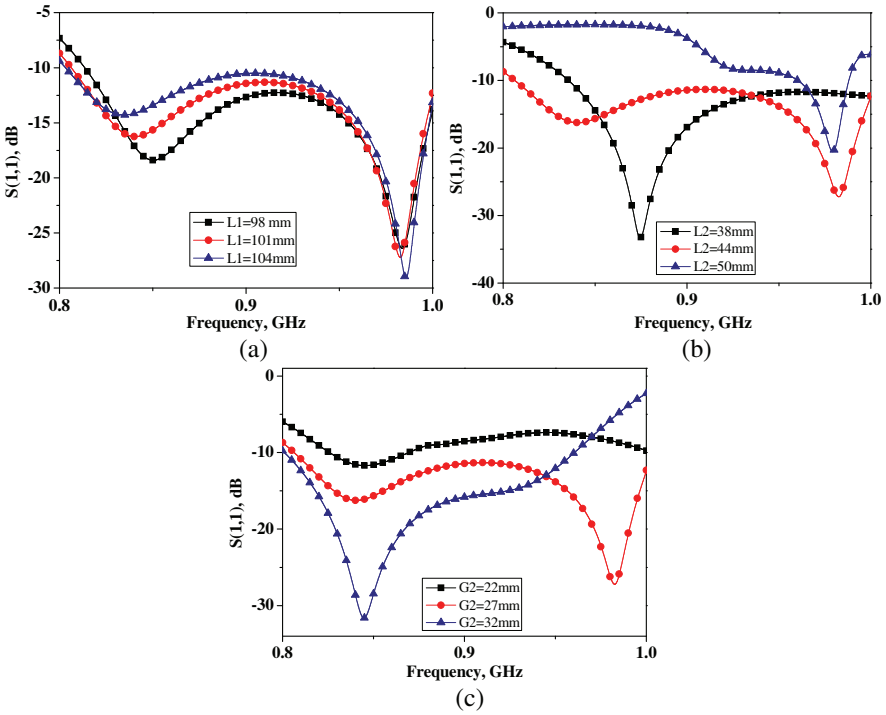

Figure 5. Reflection coefficients for different values of $L1$, $L2$ and $G2$. (a) $L1$, (b) $L2$, (c) $G2$.

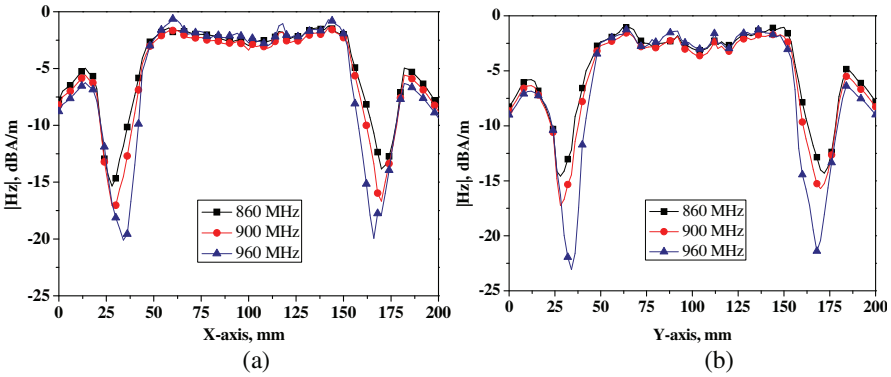

Figure 6. Simulated |Hz| (dBA/m) along X and Y-axis of the proposed antenna when $Z = 10$ mm. (a) X-axis, (b) Y-axis.

Calculated and optimized parameters of the feedline are: $W1 = 5$ mm, $W2 = 3.5$ mm, $G1 = 48$ mm.

Reflection coefficients for different values of $L1$, $L2$ and $G2$ are analyzed in Figs. 5(a)–(c). In Fig. 5(a), the impedance bandwidth shifts down as the value of $L1$ is increased from 98 mm to 104 mm. As seen in Fig. 5(b), when parameter $L2$ is set 38 mm or 50 mm, the impedance bandwidth becomes narrow, and good impedance matching cannot be achieved. To obtain broadband performance, $L2$ is optimized to 44 mm. Apart from this, Fig. 5(c) exhibits reflection coefficients for different values of $G2$. When $G2$ gets large or small, broadband performance is influenced. So parameter $G2$ is set to 27 mm.

Figure 6 plots the vertical magnetic field strength distributions |Hz| (dBA/m) along X-axis and Y-axis at the height of 10 mm above the antenna when frequency is operating at 860 MHz, 900 MHz and 960 MHz. The strength of magnetic field is about -2.5 dBA/m in the interrogation zone (50 mm$\leq X \leq$ 150 mm, 50 mm$\leq Y \leq$ 150 mm). Variation of field is below 0.5 dBA/m. Simulated results indicate that strong and uniform distribution of magnetic field is generated among the square area formed by multiple-arm dipoles, and the antenna also achieves broadband between 860 MHz–960 MHz.

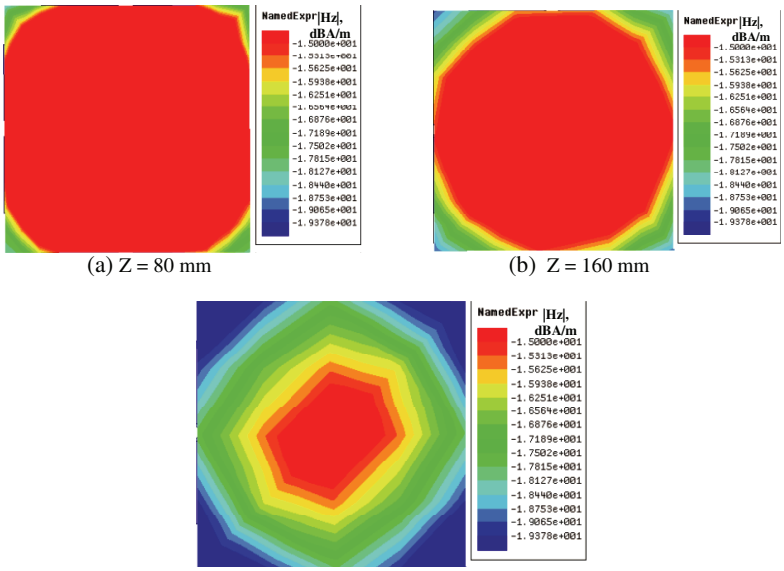

(a) Z = 80 mm (b) Z = 160 mm

(c) Z = 240 mm

Figure 7. $|Hz|$ (dBA/m) distribution at different heights (a) $Z = 80\,\text{mm}$, (b) $Z = 160\,\text{mm}$, (c) $Z = 240\,\text{mm}$.

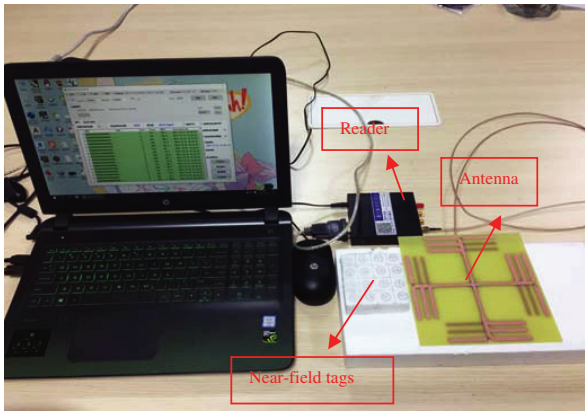

Figure 8. Measurement on read range.

Simulated magnetic field distribution of interrogation zone ($140 \times 140\,\text{mm}^2$) is shown in Fig. 7. The height is separately at $Z = 80\,\text{mm}$, 160 mm, 240 mm, and the excitation power is set 30 dBm. By increasing the height of zone from antenna surface, strength of magnetic field is lowered. When the height is at 80 mm and 160 mm, the magnetic field is up to $-15\,\text{dBA/m}$ in the whole region. Even when the height is at 240 mm, the magnetic field strength is still above $-20\,\text{dBA/m}$. The magnetic field is enhanced obviously compared to single-arm dipole array.

To verify the performance of the multiple-arm dipole antenna array, the antenna has been integrated into a commercial desktop reader, and read range tests have been carried out. Measured system is set up in Fig. 8. In this test, the near-field tag (Impinj J41, field strength at least $-24\,\text{dBA/m}$,) and Imping Speedway Revolution reader R220 are chosen. The J41 tag is a commercial Monza 4 microchip tag using a 6-mm-radius (out radius) loop antenna. The read sensitivity of the chip is 17.4 dBm. Identifying the tag J41 requires the component of the magnetic field (normal to the surface of the antenna) to be at least $-24\,\text{dBA/m}$. The antenna surface ($100 \times 100\,\text{mm}^2$) is subdivided into 5×5 square cells. Detection tests are repeated in each cell by varying the distance of the tag from antenna surface, setting an input power to 25 dBm. The measured heights are separately set to 80 mm (Fig. 9(a)), 160 mm (Fig. 9(b))

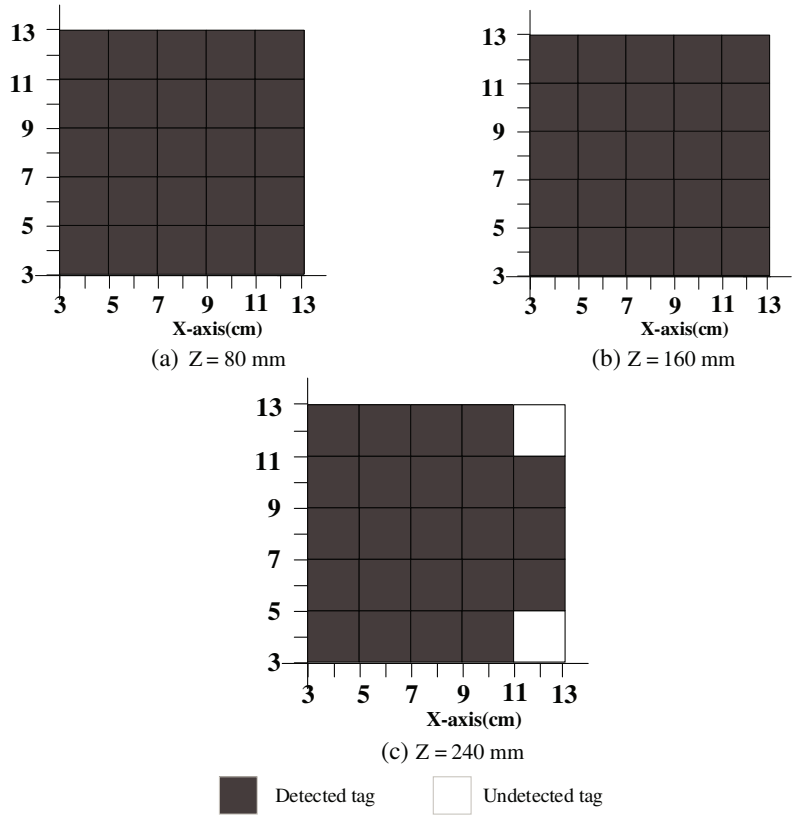

Figure 9. Tag detection test for NF tag, by varying distance, position with respect to antenna surface (a) $Z = 80\,\text{mm}$, (b) $Z = 160\,\text{mm}$, (c) $Z = 240\,\text{mm}$.

and 240 mm ((Fig. 9(c)). By observing the detection of tags, the 100% reading rate is up to almost 200 mm, and large reading region is exhibited.

3. CONCLUSION

In this letter, a multiple-arm dipole antenna array fed by a quarter-wave double-side parallel stripline (QDSPSL) structure has been proposed for NF-UHF RFID desktop reader applications. Broadband performance is achieved by different resonant frequencies. Magnetic distribution is maximized in a confined volume close to antenna surface, and field uniformity is obtained in UHF band. Large reading region of $100 \times 100\,\text{mm}^2$ and 100% reading rate up to 200 mm for NF tags are exhibited. The antenna has a good prospect in UHF RFID near-field applications.

ACKNOWLEDGMENT

This work is supported by Aviation Science Foundation Project (Grant 20161852017).

REFERENCES

1. Michel, A., R. Caso, A. Buffi, P. Nepa, and G. Isola, "Modular antenna for reactive and radiative near-field regions of UHF-RFID desktop reader," *IEEE General Assembly and Scientific Symposium*, 1–4, 2014.
2. Ahmad, M. Y. and A. S. Mohan, "Novel bridge-loop reader for positioning with HF RFID under sparse tag grid," *IEEE Transactions on Industrial Electronics*, Vol. 61, No. 1, 555–566, 2013.

3. Ding, X. M., K. Zhang, H. Yu, and L. Zhu, "A novel magnetic coupling UHF near field RFID reader antenna based on multilayer-printed-dipoles array," *IEEE Transactions on Magnetics*, Vol. 50, No. 1, 1–4, 2014.
4. Shi, J., X. Qing, and Z. N. Chen, "Electrically large zero-phase-shift line grid-array UHF near-field RFID reader antenna," *IEEE Transactions on Antennas and Propagation*, Vol. 62, No. 4, 2201–2208, 2014.
5. Li, X. and Z. Yang, "Dual-printed-dipoles reader antenna for UHF near-field RFID applications," *IEEE Antennas and Wireless Propagation Letters*, Vol. 10, No. 1, 239–242, 2011.
6. Zheng, J., C. Zhou, Y. Yang, X. He, and C. Y. Mao, "QDSPSL-fed straight dipoles antenna array for UHF RFID near-field applications," *Progress In Electromagnetics Research Letters*, Vol. 72, 107–112, 2018.
7. Wei, X. D., H. L. Zhang, and B. J. Hu, "Novel broadband center-fed UHF near-field RFID reader antenna," *IEEE Antennas and Wireless Propagation Letters*, Vol. 14, 703–706, 2015.
8. Zheng, J., Y. Yang, X. He, and C. Y. Mao, "A CP Antenna of wide half-power beamwidth for UHF RFID near- and far-field applications," *Progress In Electromagnetics Research Letters*, Vol. 72, 61–67, 2018.
9. Cho, C., J. Ryoo, I. Park, and H. Choo, "Design of a novel ultra-high frequency radio-frequency identification reader antenna for near-field communications using oppositely directed current," *IET Microwaves Antennas and Propagation*, Vol. 4, No. 10, 1543–1548, 2010.
10. Cho, C., C. Lee, J. Ryoo, and H. Choo, "Planar near-field RFID reader antenna for item-level tagging," *IEEE Antennas and Wireless Propagation Letters*, Vol. 10, No. 11, 1100–1103, 2011.
11. Pakkathillam, J. K. and M. Kanagasabai, "A novel UHF near-field RFID reader antenna deploying CSRR elements," *IEEE Transactions on Antennas and Propagation*, Vol. 65, No. 4, 2047–2050, 2017.
12. Daiki, M. and E. Perret, "Near-field modular antenna concept with configurable reading area for RFID applications," *IEEE Transactions on Antennas and Propagation*, Vol. 65, No. 3, 1015–1025, March 2017.